



Project no. **SES6-CT-2004-502824**

Project acronym: **CROPGEN**

Project title: **Renewable energy from crops and agrowastes**

Instrument: Specific Targeted Research Project

Thematic Priority: SUSTDEV: Sustainable Energy Systems

D27: Mathematical description of the AD process with high solids feedstocks for design purposes

Due date of deliverable: Month 36
Actual submission date: Month 36

Start date of project: 01/03/2004

Duration: 39 months

Organisation name of lead contractor for this deliverable

Wageningen University (WU)

Revision [0]

Project co-funded by the European Commission within the Sixth Framework Programme (2002-2006)		
Dissemination Level		
PU	Public	
PP	Restricted to other programme participants (including the Commission Services)	PP
RE	Restricted to a group specified by the consortium (including the Commission Services)	
CO	Confidential, only for members of the consortium (including the Commission Services)	

D27: Mathematical description of the AD process with high solids feedstocks for design purposes

This deliverable consists of two main sections: section 1 describes the practical work carried out by WU to determine hydrolysis kinetics from anaerobic digestion processes fed with energy crops and co-substrates, while section 2 explains how this is implemented in the model Anaerobic Digestion Model 1 (ADM1) which serves as a basis for the Virtual Laboratory developed by BOKU-IAM as part of the CROPGEN project.

Section 1: Hydrolysis kinetics from AD processes fed with energy crops and co-substrates

1.1 Introduction

Hydrolysis can be defined as the breakdown of organic substrate into smaller products that can subsequently be taken up and degraded by bacteria (Morgenroth et al 2002 in Angelidaki and Sanders, 2004). In the hydrolysis step, complex suspended compounds and colloidal matter are converted into their monomeric or dimeric components, such as aminoacids, single sugars and long chain fatty acids (LCFA). The many intervening factors and the nature of the substrate make the hydrolysis process a complex one (Mata-Alvarez et al. 2000). When digesting lignocellulosic material, hydrolysis of the complex organic matter can be regarded as the rate-limiting step (Hobson 1983; Noike et al. 1985). Therefore, understanding the hydrolysis process and assessing properly the implied parameters is of crucial importance for proper process design.

It has been shown that hydrolysis of complex wastes is mainly surface related for particulate substrates while the amount of active enzymes is rate limiting for dissolved substrates (Sanders 2001). Therefore, in the case of particulate substrates, the rate of hydrolysis (k_h) can be expressed as $\text{g COD/m}^2/\text{day}$ (Sanders et al. 2000; Song 2003). However, as for most substrates the amount of available surface is unknown, hydrolysis is usually described as a first order process with regards to the substrate concentration (Eastman and Ferguson 1981). In this empirical first order hydrolysis kinetic relation it is assumed that a change in concentration of biodegradable substrate with time (dX_{degr}/dt) is linearly related, at constant pH and temperature, to the concentration of biodegradable substrate (X_{degr}) (equation 1).

$$dX_{degr} / dt = -k_h * X_{degr} \quad (1)$$

Although the first order kinetics is an empirical relation, it does reflect the major aspect of the hydrolysis of particulate substrates, namely the fact that the hydrolysis of particles is limited by the amount of available surface. (Sanders et al. 2002; Valentini et al. 1997; Vavilin et al. 1996; Veeken and Hamelers 1999).

Already in 1983, Hobson reported that the anaerobic bacterial attack on fibres in the rumen occurs by attachment of the bacteria to the fibre and degradation of the fibres from broken ends or damaged surfaces. Therefore, a smaller particle size will not only lead to an increased total surface area but also to a higher extent of structural damage of the fibre allowing bacteria to access the degradable substrate. As such, the results of Hills and Nakano(1984) proved how the hydrolysis rate of tomato wastes increased for decreasing particle sizes.

It was however unclear if the hydrolysis mechanism was related to the enzymes being excreted in the bulk solution or to bacteria directly attached to the particle surface. In 1999, Veeken and Hamelers showed that diffusion of hydrolytic enzymes from the bulk solution to the particle surface is not the rate limiting step in hydrolysis of biowaste material because the difference in activation energy for diffusion is much lower than that for hydrolysis-related enzyme kinetics, i.e. 20 KJ/mol vs. 64 KJ/mol. Furthermore, recently Song et al. (2005) showed that hydrolysis with leachate as inoculum occurs on the outside of the cellulose particles by the action of hydrolyzing bacteria attached to the surface. Since it is assumed that particles will be completely covered with bacteria excreting the necessary enzymes, the hydrolysis rate of particulate substrate will then be related to the size of the particles or to the number of adsorption sites at the particle surface and not so much to the total amount of enzymes present.

It is known that in the microbial hydrolysis of polysaccharides, complex enzyme systems exist comprising from few to 20 or more enzymes (Warren 1996), each of them hydrolyzing particular substrates and showing different properties related to their optimum activity. Therefore, the amount of adsorption sites available for hydrolysis will not only be determined by the particle size of the substrate but also by its composition.

For the assessment of the hydrolysis kinetics, knowledge on the biodegradability of the substrate is necessary. Research has been conducted in the past with the aim of clarifying the relationships between the structural features of lignocellulosic biomass and the final biodegradability (Chandler et al. 1980; Chynoweth et al. 1993; Tong et al. 1990), however, results are not fully conclusive. Most authors have found an important relation between the lignin content of the substrate and its ultimate anaerobic biodegradability. However, the influence of cellulose and its properties has been also recognised (Buffiere et al. 2005; Tong et al. 1990), as well as the effects of other functional compounds, like hemicellulose, starch, lipids, which have been included in the models proposed by Amon (2007).

Less extensive research has been carried out relating the hydrolysis rate to substrate composition. The study by Tong et al (1990) is one of few examples. They reported a good relation between the first order methane production constant and the lignin content of eight samples ($r^2=0.82$). However, the rates reported correspond only to the methane production, hence assuming that hydrolysis was the rate limiting step. Unfortunately, intermediary products like VFA and other soluble compounds were not measured in their research so no conclusive interpretation of the results could be made. Chynoweth (1993) also found an apparent correlation between the rate of conversion and the lignin content. Later, Veeken and Hamelers (1999) found an increase in the hydrolysis rate constant at increasing biodegradability but no detailed compositional analysis of their substrates was reported.

1.2 Materials and methods

Test set-up

The ultimate biodegradability and hydrolysis rates of 15 plant samples were assessed using the oxitop protocol developed as part of D5. A sludge mixture consisting of suspended and granular sludge and an S/I ratio equal to 0.5 (VS basis) was used in order to guarantee adequate presence of hydrolytic and methanogenic microbial populations. Table 1 summarises the characteristics of the test set-up.

The fifteen plant samples used as substrate were part of the species sent as part of WP1. Plant samples were freeze dried and then ground and sieved to through a 0.2 mm sieve. Samples were fully characterised in terms of TS, VS, COD, elemental composition (CHNO), fibre analysis and starch. The substrates used and their characteristics are listed in Table 2.

Table 1. Test set-up

Input	Amounts				Concentrations	
Plant sample	1.3	g	0.34	gCOD (0.27) (gVS)	2.0	gCOD/l (1.6) (gVS/l)
Sludge Mixture Total	17.5	g	0.5	gVS	3	gVS/l
- Granular sludge	5	g	0.25	gVS		
- Digested primary sludge	12.5	g	0.25	gVS		
Macronutrients *	0.4	ml			2.5	ml/l
Trace elements *	0.2	ml			1.25	ml/l
Phosphate buffer *	8	ml			20	mM
DemiWater	140	ml				
Total liquid volume	167	ml				

The bottles were filled by adding demiwater and medium solution, followed by the sludges. Finally, when all bottles are prepared the plant sample was added. After completing the procedure, bottles were flushed with nitrogen gas for approx 30 seconds and covered with the oxi-top head equipped with a septum rubber ring to avoid leakages. The bottles were provided with adequate shaking (100 rpm) and mesophilic temperature conditions (35°C) for the duration of the experiment.

Test monitoring

In order to calculate the biodegradability and degradation rates of the plant samples, methane production along with soluble COD and VFA were monitored daily during the first week and twice per week, thereafter. The liquid samples were taken from the bottles using a syringe, and then centrifuged for ten minutes at 10000 rpm in a Microlite Therme IEC Boomlab centrifuge, the supernatant being used for the assessment.

Analytical methods

For characterisation of the substrates and sludges freeze drying was performed in liquid nitrogen in a GRI freeze drier equipped with two condensers. Comminution was performed in a Retsch BV grinder (Haan, Germany). TS, VS were performed according to standard methods (APHA, 1998). COD was calculated based on the elemental analysis of the materials, which was performed in a Thermoquest CE-instruments 1110 CHNS-O equipped with a prepacked quartz reactor column. Fibre analysis was performed according to van Soest (1991) using the freeze dried ground samples. All analyses were performed in duplicate. Dr. Lange kits (Düsseldorf, Germany) were used for assessing soluble COD, the samples being measured in a Dr. Lange Xion 500 model LPG-385 photo-spectrometer (Düsseldorf, Germany). VFA was analyzed in a Hewlett Packard 5890A gas chromatograph equipped with a glass column packed with Supelcoport and coated with 10% Fluorad FC 431 combined with a Hewlett Packard 6890 series injector (Palo Alto, U.S.A.). The temperatures of the flame ionisation detector, injection port and columns were 280°C, 200°C and 130°C, respectively. Gas composition was followed with a Hewlett Packard 5890A (Palo Alto, USA.) gas chromatograph. The oven, injection port and detector temperature were 45°C, 110°C and 99°C, respectively. The column measuring oxygen, nitrogen and methane was a Molselve 0.53mm x 15µm, while the column for carbon dioxide was a Paraplot 0.53mm x 20µm.

Table 2. Plant characterisation

Species	TS (gTS/gfd)	VS (gVS/gfd)	COD (gO ₂ /gVS)	Total Fibre (g/gVS)	L (g/gVS)	C (g/gVS)	H (g/gVS)	Starch (g/gVS)	Protein (g/gVS)
Yellow									
lupin	0.93	0.86	1.64	0.58	0.06	0.39	0.13	0.002	0.15
Vetch	0.93	0.86	1.47	0.512	0.08	0.30	0.13	0.026	0.18
Carrot	0.88	0.79	1.37	0.291	0.01	0.18	0.11	0.000	0.18
Spartina	0.94	0.83	1.42	0.772	0.07	0.25	0.46	0,000	0.12
White									
lupin	0.93	0.86	1.46	0.655	0.02	0.33	0.30	0.013	0.21
Triticale	0.94	0.90	1.43	0.468	0.03	0.23	0.21	0.316	0.08
Bracken	0.93	0.88	1.51	0.627	0.19	0.33	0.11	0.047	0.20
Sweet									
clover	0.93	0.84	1.58	0.528	0.03	0.32	0.18	0.000	0.17
Winter									
Barley	0.94	0.90	1.43	0.646	0.02	0.23	0.40	0.220	0.09
Winter									
bean	0.92	0.84	1.52	0.415	0.05	0.21	0.15	0.011	0.26
Sweet pea	0.90	0.81	1.53	0.289	0.03	0.19	0.07	0.111	0.24
Oil seed									
rape	0.94	0.87	1.62	0.543	0.08	0.31	0.15	0.022	0.13
Buckwheat	0.93	0.84	1.45	0.439	0.07	0.24	0.12	0.038	0.14
Rosebay									
willow	0.93	0.87	1.53	0.765	0.09	0.40	0.14	0.015	0.15
Quinoa	0.94	0.83	1.30	0.274	0.01	0.13	0.23	0.192	0.13

L: Lignin; C: Cellulose; H: Hemicellulose.

1.3 Calculations

Biochemical Methane Potential

The BMP, expressed as litres methane at standard temperature and pressure per amount of substrate volatile solids added ($\text{ICH}_4\text{-STP. gVS}^{-1}$), is calculated from the net maximum methane production of the sample bottle corrected by the maximum methane production of the blank bottle. The maximum moles of methane produced is calculated by applying the ideal gas equation to the total pressure increase and multiplying the biogas moles by the percentage of methane in the headspace. Such amount is transformed to litres methane by multiplying by 22.4 which is the volume of one mol of gas at STP conditions. (Equation 2).

$$BMP = \frac{\left[\left[\frac{(P_s + P_{atm}) * V}{R * T} \right] * \%CH_{4s} \right] - \left[\left[\frac{(P_{bl} + P_{atm}) * V}{R * T} \right] * \%CH_{4bl} \right]}{S_o} * 22.4 \quad (2)$$

Where P_s is the pressure in sample bottle (Pa), P_{atm} is the atmospheric pressure (Pa), P_{bl} is the pressure in blank bottle (Pa), V is the headspace volume (m^3), T is the temperature ($308.16 \text{ }^\circ\text{K}$), R is the universal gas constant ($8.3114 \text{ Pa m}^3 \text{ mol}^{-1} \text{ }^\circ\text{K}^{-1}$), $\%CH_{4s}$ is the percentage methane in sample bottle, $\%CH_{4bl}$ is the percentage methane in the blank bottle and S_o is the amount of substrate added (gVS).

Hydrolysis rate

As described previously the hydrolysis rate in anaerobic systems can be described as first-order with respect to the concentration of degradable particulate organic matter (equation 1). The calculation of the hydrolysis rate in batch reactors is done using equation 3 which relates the first order hydrolysis constant, the digestion time and effluent concentration (Sanders 2001).

$$X_{ss,t=t} = X_{ss,t=0} \cdot (1 - f_h) + f_h \cdot X_{ss,t=0} \cdot e^{-k_h t} \quad (3)$$

For the estimation of the first order hydrolysis rate constant, equation 3 can be linearised to give equation 4.

$$\ln\left(\frac{X_{ss,t=t} - X_{ss,t=0} \cdot (1 - f_h)}{X_{ss,t=0} \cdot f_h}\right) = -k_h t \quad (4)$$

Where $X_{ss,t=t}$ is the concentration of particulate substrate in the bottle at time t (Biodegradable + non biodegradable) (gCOD/l), $X_{ss,t=0}$ is the concentration of particulate substrate at time $t=0$ (Biodegradable + non biodegradable) (gCOD/l), f_h is the biodegradable fraction of particulate substrate, $0 < f_h < 1$, k_h is the first order hydrolysis constant (d^{-1}) and t is the batch digestion time (day). In all cases, calculation of X_{ss} is done by subtracting the total COD solubilised (soluble COD plus COD methanised at time t) from the total plant COD added at the start up.

The ultimate biodegradability of the particulate material f_h was calculated by using equation 5.

$$f_h = \left(\frac{COD_{methane,t=\infty} + COD_{s,t=\infty} - COD_{s,t=0}}{gCOD_{in} - COD_{s,t=0}} \right) \quad (5)$$

Where: COD_{methane, t=∞}: COD equivalent of methane produced at final digestion time
 COD_{s, t=∞}: soluble COD at final digestion time
 COD_{s, t=0}: soluble COD at time t=0
 g COD_{in}: initial amount of COD in the influent

Both biodegradability and conversion rates are affected by the concentration of intermediates in the blank, therefore, for all calculations presented, net values are used, that is after subtraction of the blank values.

1.4 Results

Table 3 presents the BMP, biodegradability and hydrolysis rates calculated for the tested materials. Relationships were established between the plant composition and the final biodegradability assessed (Figure 1). The lignin content, although low in absolute quantity, is strongly related to the amount of COD converted to methane. Still, the strongest correlation was found between the content of lignin plus cellulose and the amount of methane generated from the plant biomass. The latter correlation can be used to roughly estimate the CH₄ production (or BMP) of new plant species of which the fibre composition is known:

$$m^3 \text{ CH}_4\text{-prod. (STP)/kg plant COD added} = 0.31 - 0.34 \cdot F_{L+C} \quad (6)$$

in which F_{L+C} = total amount of lignin and cellulose per g plant VS.

Table 3. Biodegradability and hydrolysis constants assessed from batch experiments

Species	BMP l CH ₄ gVS ⁻¹	BMP l CH ₄ gCOD ⁻¹	COD methanised (%) ^a	kh (day ⁻¹)	fh (%) ^b
Yellow lupin	0.26	0.16	45%	0.49	36
Vetch	0.29	0.20	56%	0.47	43
Carrot	0.31	0.23	66%	0.61	31
Spartina	0.29	0.21	59%	0.22	52
White lupin	0.26	0.18	52%	0.43	35
Triticale	0.29	0.20	57%	0.43	52
Bracken	0.18	0.12	34%	0.24	22
Sweet clover	0.29	0.18	53%	0.54	42
Winter					
Barley	0.30	0.21	60%	0.32	51
Winter bean	0.35	0.23	66%	0.66	55
Sweet pea	0.37	0.24	70%	0.72	61
Oil seed rape	0.29	0.18	51%	0.48	59
Buckwheat	0.32	0.22	63%	0.48	54
Rosebay					
willow	0.20	0.13	37%	-	-
Quinoa	0.33	0.25	72%	-	-

a: Proportion of Total COD converted into methane by the end of the digestion time.

b: Proportion of the particulate COD that was solubilised by the end of the digestion time.

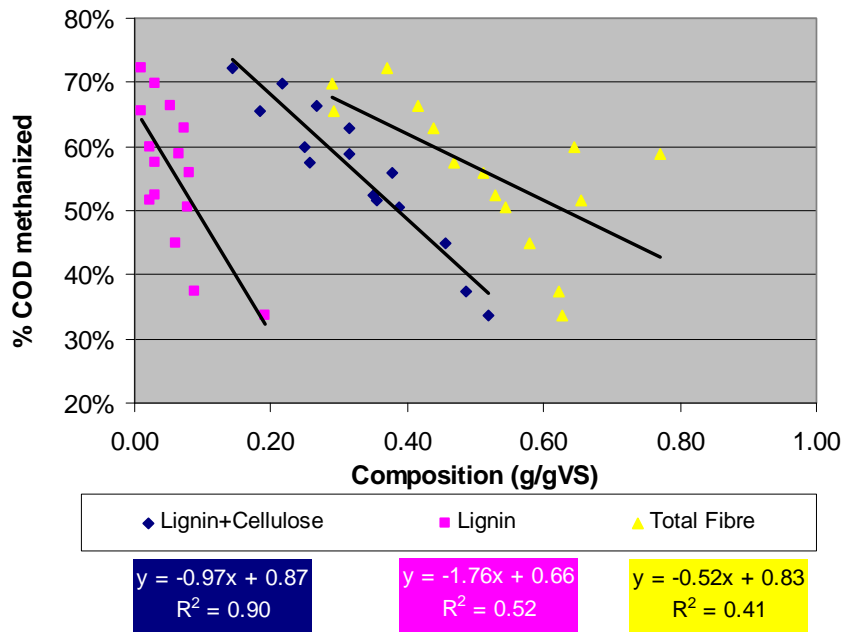


Figure 1. Percentage methanised COD in dependence of substrate composition

Hydrolysis rates calculated were also related to the initial composition of the plant material being digested (Figure 2). Hydrolysis rates assessed were found to be better correlated to the total fibre content of the plant material, while relation with lignin alone was found not to be significant. This suggests that the overall matrix formed by the association of cellulose, hemicellulose and lignin would account for the rate of degradation of the particulate material in the plant samples.

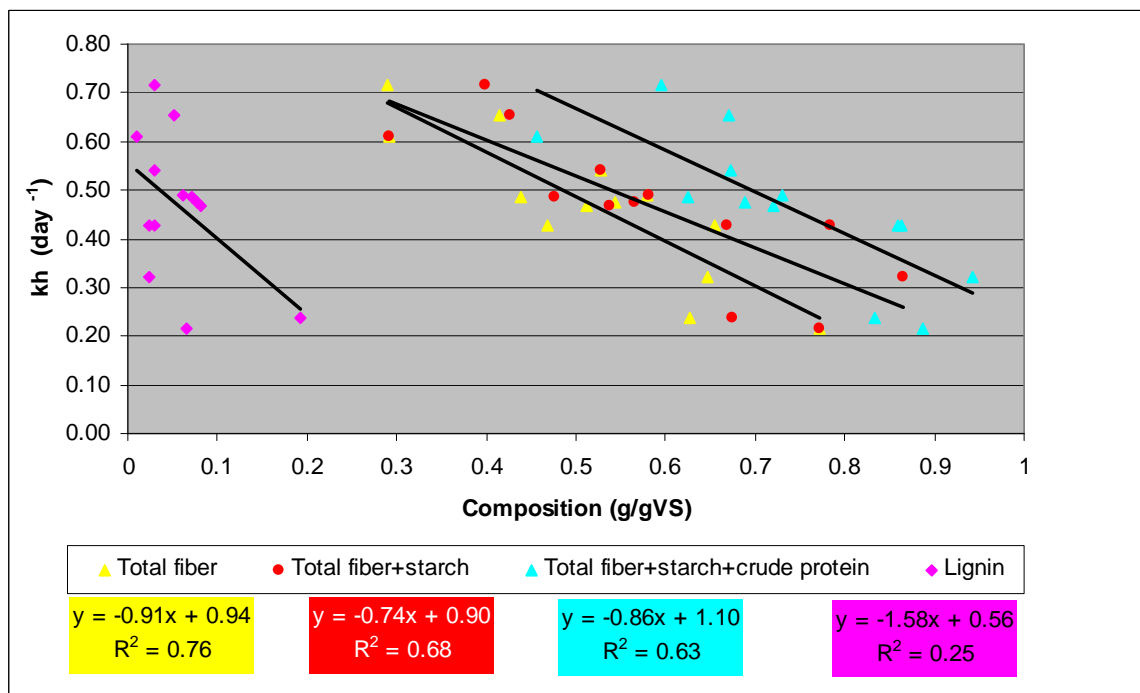


Figure 2. Hydrolysis rates in dependence of substrate composition

The degradation of the plant material was studied in more detail in seven of the fifteen digested plant species. A simplified first order model was first used and then compared to a more complex model in which three types of material were simulated to be degraded at different rates, namely: biodegradable soluble material, fast biodegradable particulate material and slow biodegradable particulate material.

The fraction of biodegradable soluble material (f_s) is calculated following equation 7 (Conventions as in equation 5).

$$f_s = \frac{COD_{s,t=0} - COD_{s,t=\infty}}{COD_{s,t=0}} \quad (7)$$

The fractions of fast and slow degradable particulate material were calculated following the COD diagram presented in Figure 3. It was assumed that the fraction of non fibre degradable fraction of the plant material (nfbCOD) correspond to the sum of the fractions of starch, crude protein and other non fibre particulate in the sample. Following, and considering the fraction of particulate biodegradable material (pbCOD) known from equation 5, the amount of biodegradable fibre is calculated as the difference among the two values (fbCOD=pbCOD-nfbCOD). The model then considers the nfbCOD to be the fast degradable material, while the fbCOD correspond to the slow degradable material.

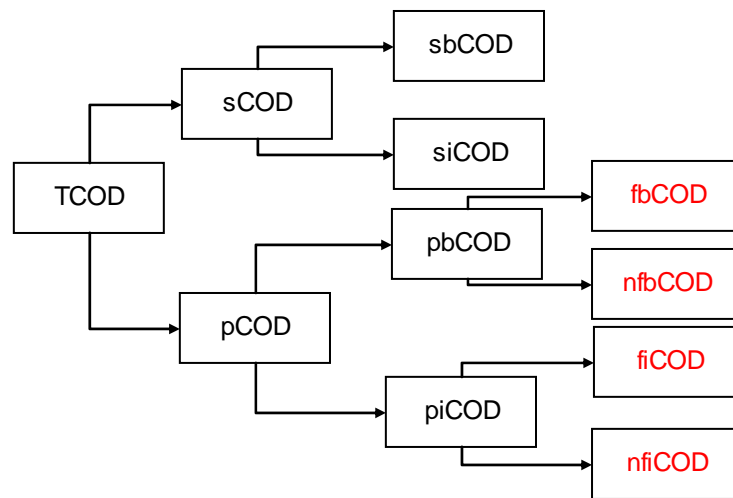


Figure 3. COD scheme showing the fractions considered for the model developed
T = Total; s = soluble; p = particulate; b = biodegradable; i = inert; f=fibre; nf= non fibre

The model considers a first order degradation for the three fractions. Hence, the concentration of remaining biodegradable COD at any time t can be calculated from equation 9.

$$bCOD_{t=t} = fbCOD * e^{-k_{slow}*t} + nfbCOD * e^{-k_{fast}*t} + sbCOD * e^{-k_s*t} \quad (9)$$

Using a simplified solver tool (Microsoft Excel software), the rates k_{slow} , k_{fast} , and k_s are estimated by minimizing the sum of squares of the difference between the estimated and the measured values. The results of the estimation are presented in Figure 4.

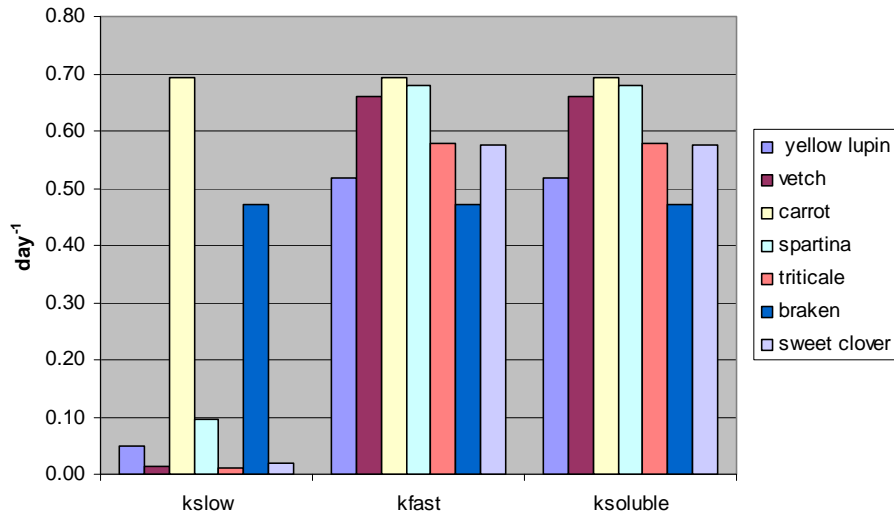


Figure 4. Estimated first order constants for the time phased kinetic model.

As presented in Figure 4, in all cases the same rate of degradation was estimated for the soluble and fast degradable particulate COD, suggesting that these fractions would behave as a single fraction during their degradation. A distinctly different rate of degradation for the slow and fast material was found for species tested, except in the cases of carrot and bracken. Both species are particular in terms of their composition, being them the highest and slowest degradable among all plant species, respectively. In addition, carrot possesses the major fraction of soluble material and bracken the major portion of lignin. The fact that slow and fast are the same for both species could then mean that the whole of their constituting material behaves as a single component due to the high portion of soluble material and low lignin content in the first case, and to the complexity of the lignocellulosic matrix in the second case.

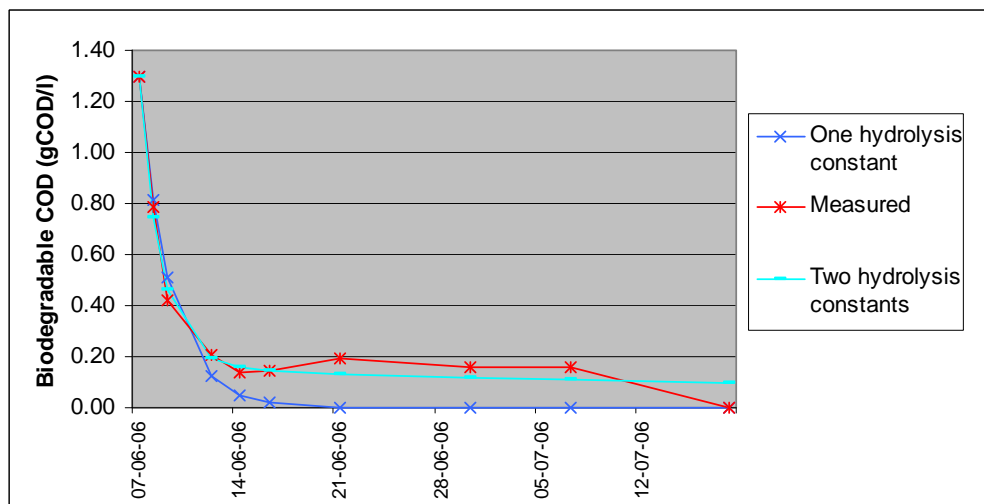


Figure 5. Measured and modelled results showing the anaerobic degradation of the biodegradable COD of an example plant specie (vetch)

Omitting the results for these two mentioned species an average first order constant for the slow digestible fraction of 0.04 day^{-1} is found and an average first order constant for the soluble and fast degradable fraction equal to 0.74 day^{-1} . Modelling the degradation of

plant material with the proposed model versus a single first order constant shows slight improvement if comparing the residual error, which in average was found to be 0.04 and 0.12, respectively (Figure 5).

The results presented are an indication of the distinct kinetic properties of the plant material during their anaerobic degradation. New models considering the surface relationship between lignin and cellulose and hemicellulose are currently under development. It is important to stress that these constants could be applicable only to material undergoing similar digestion conditions, i.e. stable neutral pH, 0.2 mm average particle size , since hydrolysis kinetics are very much susceptible to differences in test conditions, as previously mentioned.

Section 2: Implementation of AD process with high solids feedstocks in ADM1

The objective of this section of the deliverable was the further development of an existing Anaerobic Digestion (AD) model, to simulate substrates with a high solid concentration, for example energy crops. For this purpose the Anaerobic Digestion Model No. 1 (ADM1) (Batstone et al. 2002a and b) was extended with a second hydrolysis rate for slow degrading carbohydrates and the sulphate reduction process (Strik 2004). This adapted model serves as basis for the Virtual Laboratory (VL, Deliverable 16), too.

2.1 Anaerobic Digestion Model No.1 (ADM1)

The Anaerobic Digestion Model No.1 was developed by the IWA Task group for Mathematical Modelling of Anaerobic Digestion Processes. The model was presented at the 9th IWA Anaerobic Digestion Conference in Belgium in 2001 (Strik 2004).

Structure of ADM1

The model is structured in several steps characterising biochemical processes (Figure 6), such as disintegration of complex particulates to carbohydrates, proteins and lipids and the following hydrolysis to monosaccharides, amino acids and long chain fatty acids (LCFA). Subsequently the degradation of sugars and amino acids to volatile fatty acids (VFAs), hydrogen and carbon dioxide by acidogens; the acetogenesis from LCFAs and VFAs to acetate and methanogenesis from acetate and hydrogen to methane. The physico-chemical processes described are acid-base reactions and liquid gas transfer (Batstone et al. 2002a and b).

Inhibition functions imply pH, hydrogen and free ammonia. Additionally uptake-regulating functions are: competitive uptake of butyrate and valerate and secondary Monod-kinetics for inorganic nitrogen (to prevent growth under nitrogen limitations). The Task group showed also the implementation of the model in a continuous-flow stirred-tank reactor (CSTR) system, which is the most commonly used application for agricultural biogas plants (Batstone et al. 2002 a and b).

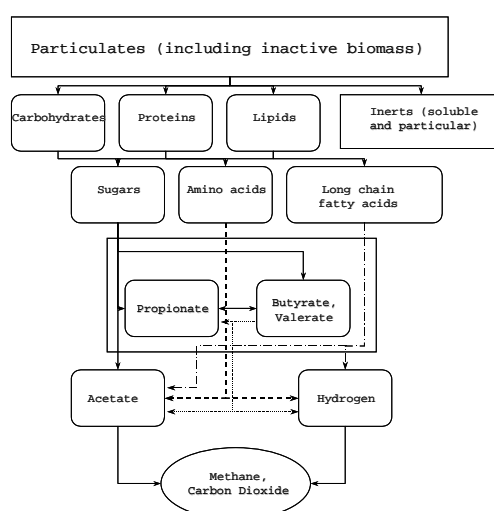


Figure 6: Biochemical processes of the anaerobic model (adapted from Batstone et al. 2002b)

Advantages and Disadvantages of ADM1

ADM1 was intended to be the first generalised model of anaerobic digestion. The model should serve as a "common basis for further model development and validation studies to make outcome more comparable and compatible" and should moreover be "assisting technology transfer from research to industry" (Batstone et al. 2002). The overall amount of required data is lower compared to neural networks. It is also more easily transferable to various applications than neural networks. The model describes process details - thus it is possible to follow the steps of the process and change single parameters. There is also the possibility to implement ADM1 in a simplified version of the model as a control tool (Strik 2004). But some disadvantages can be found as well: For effective use of the model it is necessary to understand the process. Furthermore ADM1 simplifies the AD process. As the process is very complex it is not possible to build a deterministic model without simplifications (Wilcox et al. 1995). Moreover a detailed substrate definition is required (Kleerebezem and Van Loosdrecht 2004).

Exclusions from ADM1

The model does not specify all mechanisms involved in anaerobic digestion, for instance solid precipitation, homoacetogenesis, glucose alternative products, sulphate reduction and sulphide inhibition, nitrate, weak acid and base inhibition, LCFA inhibition and acetate oxidation (Batstone et al. 2002a and b), but encourages the extension and development of it (Strik 2004).

2.2 Modification of ADM1

The original ADM1 was expected to serve as common basis for a broad range of different applications of the AD process. This resulted in a very general model. There is also a lack in some areas: For example, no analysis and validation data of the suggested biological parameters exist, especially for different feeds and reactor designs. Moreover, less information is given on the changes of kinetics for different temperature ranges (Batstone et al. 2002). Under considerations of these problems, the model is adapted for the use of energy crops in the biogas plants.

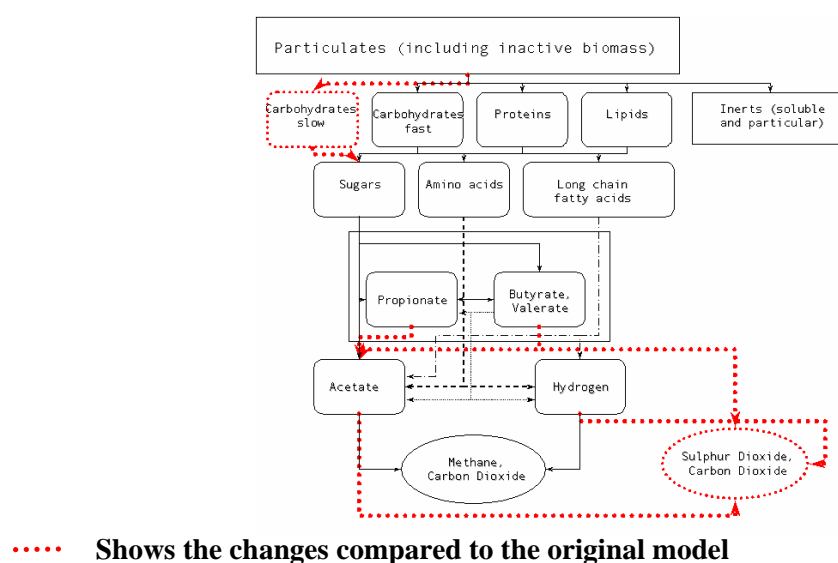


Figure 7. Schema of the biochemical processes of the adapted model

The modification of the model (Figure 7) comprises the consideration of an increased solid and cellulose content of substrates and the sulphate reduction process (Strik 2004). The high solid input – usual for energy-crop biogas plants - is considered in the input and the high cellulose content is taken into account by a second hydrolysis rate (slow and fast degradable material).

Extension of ADM1 with a second hydrolysis rate:

Process rate

$$\rho_{28} = k_{hyd_ch_s} * X \quad (10)$$

Water phase equation:

Differential equation of particulate matter:

$$\frac{dX_1}{dt} = \dots + \rho_{28} + \dots \quad (11)$$

$$\frac{dX_{47}}{dt} = \frac{q_{in}}{V_{liq}} * (X_{in,28} - X_{47}) + f_{chs,xc} * \rho_1 - \rho_{28} \quad (12)$$

Extension of ADM1 with sulphate reducing processes (according to (Fedorovich et al. 2003) implemented in (Strik 2004))

Process rates

$$\rho_{20} = \frac{k_{m,so4bu} \cdot S_{bu}}{K_{s,so4bu} + S_{bu}} \cdot \frac{S_{so4}^{2-}}{K_{so4bu} + S_{so4}^{2-}} \cdot X_5 \cdot I_{pH,13} \cdot I_{h2s,x5} \quad (13)$$

$$\rho_{21} = \frac{k_{m,so4pr} \cdot S_{pr}}{K_{s,so4pr} + S_{pr}} \cdot \frac{S_{so4}^{2-}}{K_{so4pr} + S_{so4}^{2-}} \cdot X_6 \cdot I_{pH,13} \cdot I_{h2s,x6} \quad (14)$$

$$\rho_{22} = \frac{k_{m,so4ac} \cdot S_{ac}}{K_{s,so4ac} + S_{ac}} \cdot \frac{S_{so4}^{2-}}{K_{so4ac} + S_{so4}^{2-}} \cdot X_7 \cdot I_{pH,13} \cdot I_{h2s,x7} \quad (15)$$

$$\rho_{23} = \frac{k_{m,so4h2} \cdot S_{h2}}{K_{s,so4h2} + S_{h2}} \cdot \frac{S_{so4}^{2-}}{K_{so4h2} + S_{so4}^{2-}} \cdot X_8 \cdot I_{pH,13} \cdot I_{h2s,x8} \quad (16)$$

$$\rho_{24} = k_{dec,x5} \cdot X_5 \quad (17)$$

$$\rho_{25} = k_{dec,x6} \cdot X_6 \quad (18)$$

$$\rho_{26} = k_{dec,x7} \cdot X_7 \quad (19)$$

$$\rho_{27} = k_{dec,x8} \cdot X_8 \quad (20)$$

$$\rho_{r,11} = k_{La}(S_{h2s} - 64K_{H,h2s}p_{gas,h2s}) \quad (21)$$

Process inhibition

$$I_{pH,13} = \frac{1 + 2 \times 10^{0.5(pH_{LL} - pH_{UL})}}{1 + 10^{(pH - pH_{UL})} + 10^{(pH_{LL} - pH)}} \quad (22)$$

$$I_{h2s,14-24} = 1 - \frac{S_{h2s}}{K_{l,h2s}} \quad (23)$$

Water Phase equation:

Differential equations soluble matter

$$\frac{dS_{so4^{2-}}}{dt} = \frac{q^{in}}{V_{liq}} (S_{so4^{2-}, in} - S_{so4^{2-}, out}) - 3.13e - 3\rho_{20} - 6.7e - 3\rho_{21} - 1.56e - 2\rho_{22} - 1.56e - 2\rho_{23} \quad (24)$$

$$\frac{dS_s^{2-}}{dt} = \frac{q^{in}}{V_{liq}} (S_s^{2-, in} - S_s^{2-, out}) + 0.2\rho_{20} + 0.43\rho_{21} + \rho_{22} + \rho_{23} - \rho_{A,12} \quad (25)$$

$$\begin{aligned} \frac{dS_{ac}}{dt} = & \frac{q^{in}}{V_{liq}} (S_{ac, in} - S_{ac}) + (1 - Y_{su})f_{ac, su}\rho_5 + (1 - Y_{aa})f_{ac, aa}\rho_6 + (1 - Y_{fa})0.7\rho_7 + \\ & (1 - Y_{c4})0.31\rho_8 + (1 - Y_{c4})0.8\rho_9 + (1 - Y_{pro})0.57\rho_{10} - \rho_{11} + (1 - Y_{x5})0.8\rho_{20} + (1 - Y_{x6})0.57\rho_{21} - \\ & \rho_{22} \end{aligned} \quad (26)$$

$$\frac{dS_{pro}}{dt} = \frac{q^{in}}{V_{liq}} (S_{pro, in} - S_{pro}) + (1 - Y_{su})f_{pro, su}\rho_5 + (1 - Y_{aa})f_{pro, aa}\rho_6 + (1 - Y_{c4})0.54\rho_8 - \rho_{10} - \rho_{21} \quad (27)$$

$$\frac{dS_{bu}}{dt} = \frac{q^{in}}{V_{liq}} (S_{bu, in} - S_{bu}) + (1 - Y_{su})f_{bu, su}\rho_5 + (1 - Y_{aa})f_{bu, aa}\rho_6 - \rho_9 - \rho_{20} \quad (28)$$

$$\frac{dS_{h2}}{dt} = \frac{q^{in}}{V_{liq}} (S_{h2, in} - S_{h2}) + \rho_{\dots\dots\dots} - \rho_{23} \quad (29)$$

Differential equations particulate matter:

$$\frac{dX_{x5}}{dt} = \frac{q^{in}}{V_{liq}} (X_{x5, in} - X_{x5, out}) + Y_{x5} \cdot \rho_{20} - \rho_{24} \quad (30)$$

$$\frac{dX_{x6}}{dt} = \frac{q^{in}}{V_{liq}} (X_{x6, in} - X_{x6, out}) + Y_{x6} \cdot \rho_{21} - \rho_{25} \quad (31)$$

$$\frac{dX_{x7}}{dt} = \frac{q^{in}}{V_{liq}} (X_{x7, in} - X_{x7, out}) + Y_{x7} \cdot \rho_{22} - \rho_{26} \quad (32)$$

$$\frac{dX_{x8}}{dt} = \frac{q^{in}}{V_{liq}} (X_{x8, in} - X_{x8, out}) + Y_{x8} \cdot \rho_{23} - \rho_{27} \quad (33)$$

Extra equations for Equation 19:

$$\sum_{k=1}^{12+20-24} S_k \cdot \rho_k + S_{13}(\rho_{13} + \rho_{14} + \rho_{15} + \rho_{16} + \rho_{17} + \rho_{18} + \rho_{19} + \rho_{24} + \rho_{25} + \rho_{26} + \rho_{27}) \quad (34)$$

$$S_{20} = -C_{bu} + (1 - Y_{x5})0.8C_{ac} + Y_{x5} \cdot C_{bac} \quad (35)$$

$$S_{21} = -C_{pr} + (1 - Y_{x6})0.57C_{ac} + Y_{x6} \cdot C_{bac} \quad (36)$$

$$S_{22} = -C_{ac} + Y_{x7} \cdot C_{bac} \quad (37)$$

$$S_{23} = Y_{x8} \cdot C_{bac} \quad (38)$$

Acid-base rates:

$$\rho_{A,12} = k_{A, Bhs^-} (S_s^{2-} \cdot S_h^+ - K_{a, hs} \cdot (S_{hs^-} + S_s^{2-})) \quad (39)$$

$$\rho_{A,13} = k_{A, Bh2s} (S_{hs^-} \cdot S_h^+ - K_{a, h2s} \cdot (S_{h2s} + S_{hs^-})) \quad (40)$$

Differential equations of sulphides ion states:

$$\frac{dS_{hs^-}}{dt} = \frac{q^{in}}{V_{liq}} (S_{hs^-, in} - X_{hs^-, out}) + \rho_{A,12} - \rho_{A,13} \quad (41)$$

$$\frac{dS_{h2s}}{dt} = \frac{q_{in}}{V_{liq}} (S_{h2s,in} - X_{h2s,out}) + \rho_{A,13} - \rho_{T,11} \quad (42)$$

Extension of algebraic equation:

$$\Theta = S_{cat}^+ + S_{nh4}^+ - S_{hco3}^- - \frac{S_{ac}^-}{64} - \frac{S_{pr}^-}{112} - \frac{S_{bu}^-}{160} - \frac{S_{va}^-}{208} - \frac{S_s^{2-}}{32} - \frac{S_{hs}^-}{72} - \left(\frac{S_{so4}^{2-}}{96} \cdot 2 \right) - S_{an}^- \quad (43)$$

Gas phase equations:

$$\frac{dS_{gas, h2s}}{dt} = - \frac{S_{gas, h2s} \cdot q_{gas}}{V_{gas}} + p_{T,13} \cdot \frac{V_{liq}}{V_{gas}} \quad (44)$$

$$p_{gas, h2s} = S_{gas, h2s} \frac{R \cdot T_{op}}{80} \quad (45)$$

$$q_{gas} = \dots \cdot \left(\dots + \frac{P_{T,11}}{80} \right) \quad (46)$$

Further challenges for the use of the model were the parameters suggested from the IWA Task group in the model (Table 4). The parameters quoted in ADM1 have a high margin of deviation. Moreover the suggested parameters were intended for sewage sludge as substrate and therefore not really suitable for energy crops.

Pavlostathis and Gossett (1985) found that the limiting steps in anaerobic digestion are those related to the conversion of substrate into a soluble form and the forming of methane from acetate and propionate. The IWA task-group came to a similar conclusion in the description of the Anaerobic Digestion Model No.1 (Batstone et al. 2002a and b).

Table 4. Example of parameters quoted from the IWA Task group

	Min	Max	
k_{dis}	0,25	1	$[d^{-1}]$
$k_{hyd,ch}$	0,041	106	$[d^{-1}]$
$k_{hyd,pr}$	0,0096	10	$[d^{-1}]$
$k_{hyd,li}$	0,0096	10	$[d^{-1}]$
$k_{m,su}$	4	5067	$[kg_{cod}kg_{cod}^{-1}d^{-1}]$
$k_{m,aa}$	0,5033	53	$[kg_{cod}kg_{cod}^{-1}d^{-1}]$
$k_{m,fa}$	0,6	363	$[kg_{cod}kg_{cod}^{-1}d^{-1}]$

2.3 Model Results

The differential equation system of the adapted model is solved with a differential equation (DE) solver (ODE15s Solver from MATLAB®, Version R2006b). Mathematical errors are excluded by comparing the results with the results from a second solver. The results will then be compared with measured data. If it is necessary the parameters will be adjusted until the best fit is found (Figure 8).

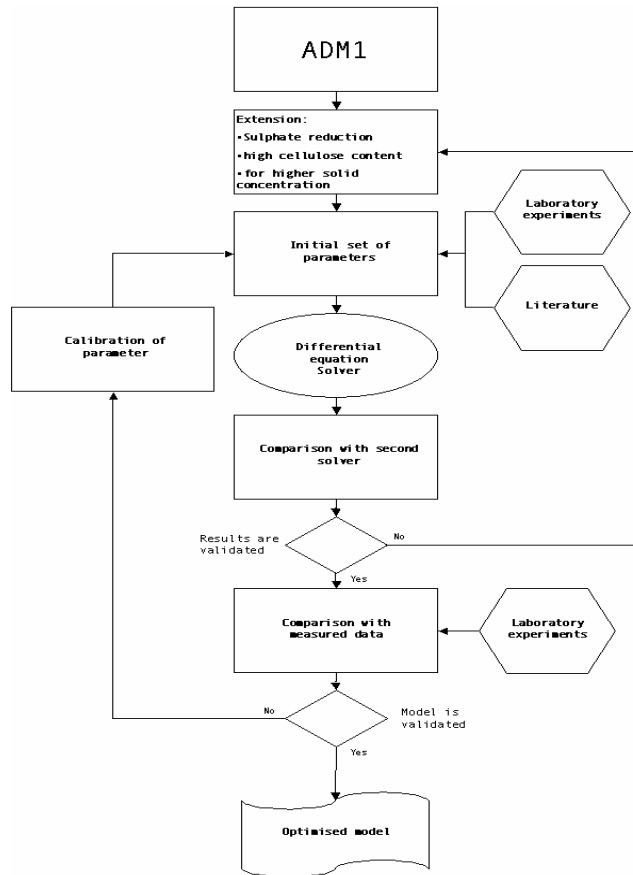


Figure 8. Optimisation Procedure for ADM1 Model

Model performance was evaluated using different statistical indicators: First of all the “most widely used statistical indicators of the goodness of fit...” (Elias et al. 2006) was used: the square of the correlation coefficient:

$$r^2 = \left(\frac{\sum_{i=1}^n (x_{pre,i} - x_{mean_pre}) * (x_{mes,i} - x_{mean_mes})}{n * \sigma_{pre} * \sigma_{mes}} \right)^2 \quad (47)$$

Moreover several other statistical indicator suggested by Elias et al. (Elias et al. 2006) were suggested, as the:

Ratio of means (Rmean):

$$R_{mean} = \frac{x_{mean_pre} - x_{mean_mes}}{x_{mean_mes}} \quad (48)$$

The total roots mean squared error (RMSE):

$$RMSE = \sqrt{\frac{\sum_{i=1}^n (x_{pre,i} - x_{mes,i})^2}{n}} \quad (49)$$

And the index of agreement (Papanastasiou et al. 2007):

$$d = 1 - \frac{\sum_{i=1}^n (x_{mes,i} - x_{pre,i})^2}{\sum_{i=1}^n (|x_{pre,i} - x_{mean_mes}| + |x_{mes,i} - x_{mean_mes}|)^2} \quad (41)$$

where:

$x_{pre,i}$	predicted values
$x_{mes,i}$	measured values
x_{mean_pre}	mean of predicted values
x_{mean_mes}	mean of measured values
σ_{pre}	standard deviation of predicted values
σ_{mes}	standard deviation of measured values
n	number of values

To gain data for model validation and calibration and also to obtain kinetic data, 4 completely stirred tank reactors (CSTR) later noted as FM1 to FM4 were operated at 35°C (mesophilic) (FM1, FM3) and at 60°C (thermophilic) (FM2, FM4). The used reactor set-up (Figure 9) was, with slight differences, developed and used at the ANERO-Control project and described by Holubar, 2003 (Holubar et al. 2003) and later also used in the AMONCO-project. We used sludge from the waste water treatment plant in Klosterneuburg, A and Altenmarkt, G as inoculum for the mesophilic reactor system; and for the thermophilic reactor system we used thermophilic sludge, also from the WWTP in Altenmarkt as inoculum.

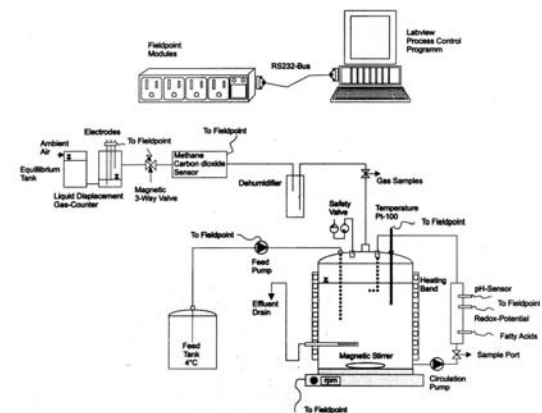
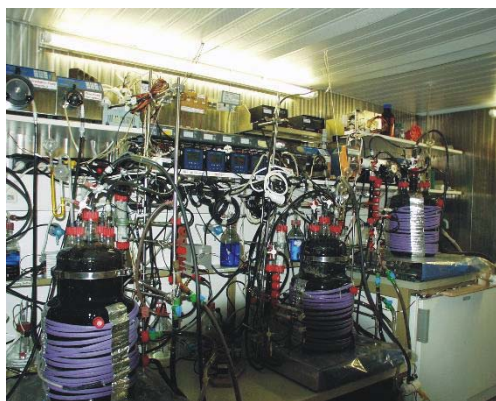


Figure 9. Scheme of the anaerobic completely stirred tank reactor

Three different substrates were used: Maize silage (only corn), whole crop silage and sunflower residues. The substrates came all from the biogas plant Pfiehl, Sitzzenberg-Reidling, Austria in different charges.

Figures 10 and 11 show some model results for the reactor system FM1 for 430 days.

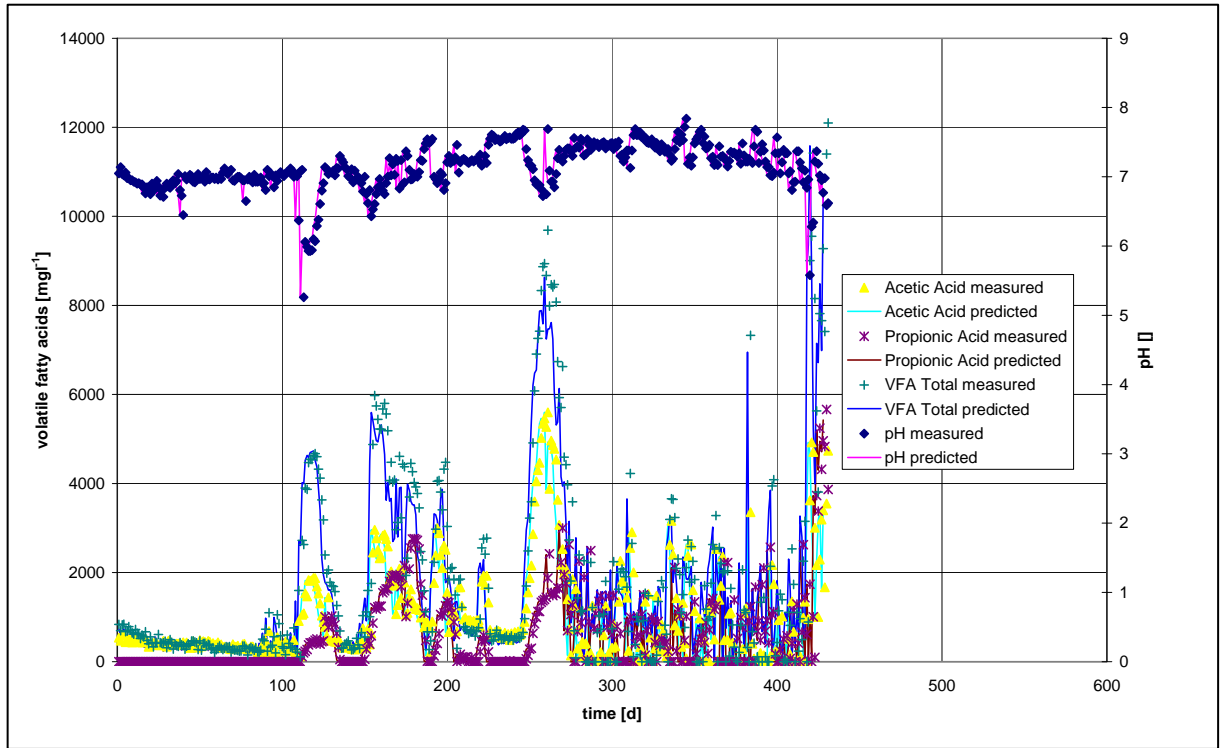


Figure 10. Model results: pH, acetic acid, propionic acid and volatile fatty acid over time

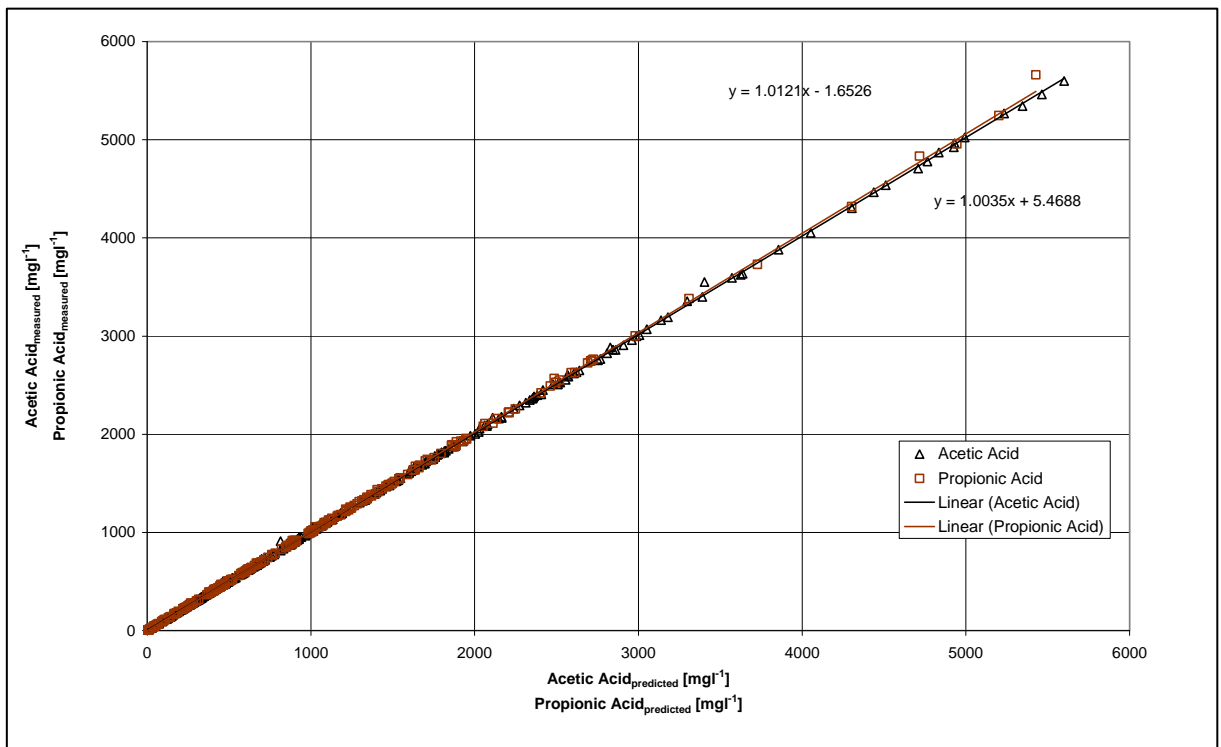


Figure 11. Model results: acetic acid and propionic acid: predicted vs. measured

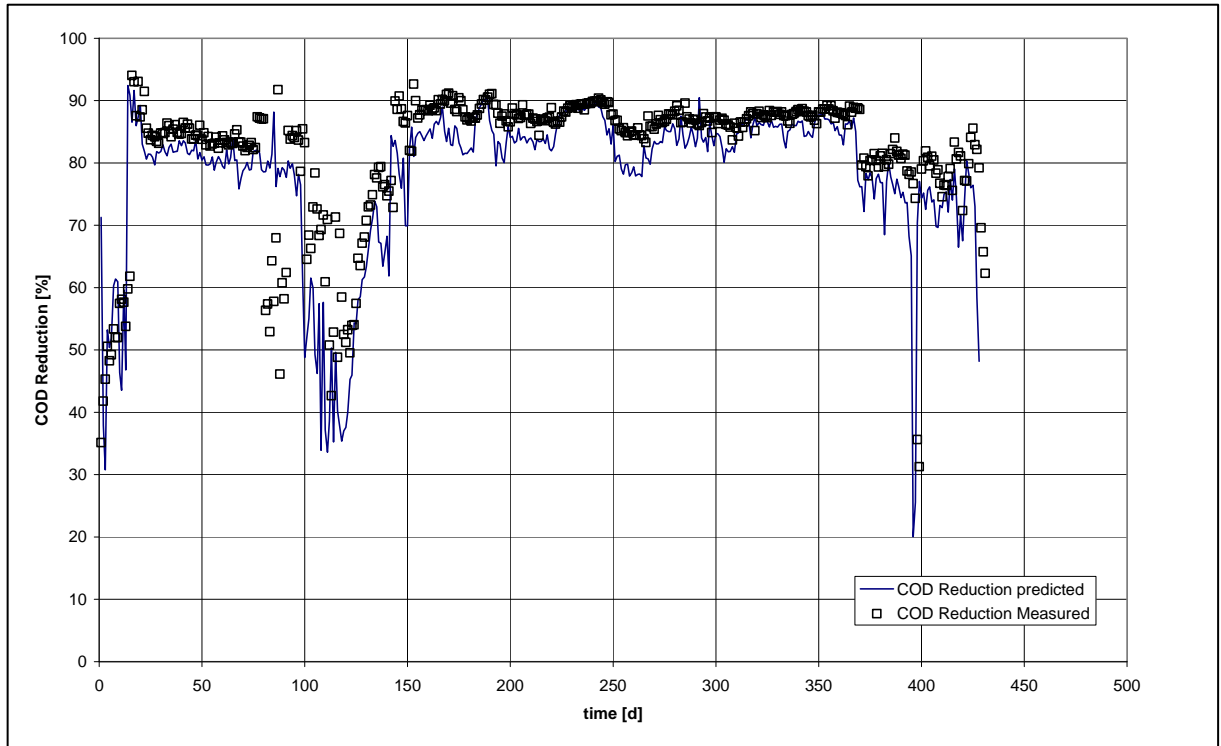


Figure 12. Model results: COD reduction over time

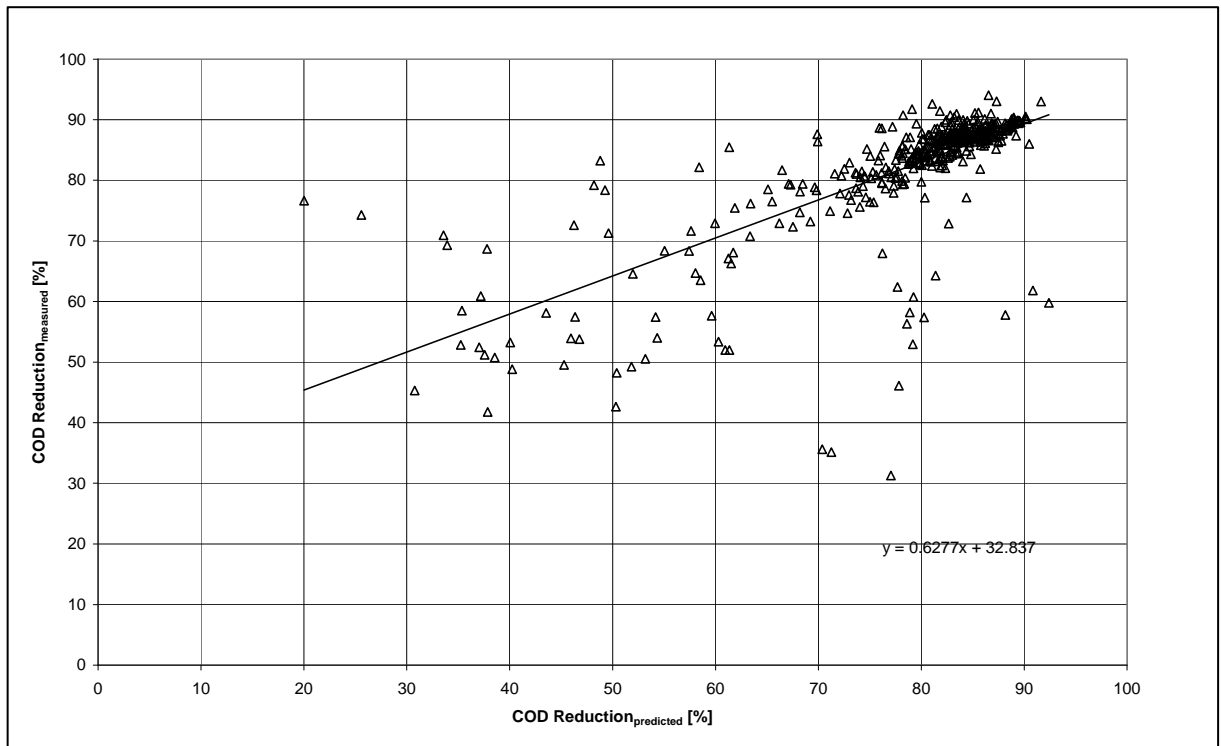


Figure 13. Model results: COD reduction: predicted vs. measured

As can be seen in Figures 10 and 11 the pH and Fatty acid concentrations were predicted very well by the model. The prediction of the gas production and the methane content was adequate (data not shown), and the prediction of COD reduction was also good (Figures 12 and 13).

The model performance for Acetic Acid concentration, Propionic Acid Concentration, Total Volatile Fatty Acids, the COD Reduction and the pH can be seen in Table 5. A correlation coefficient of 1 would describe an ideal model and a values of < 0.3 (absolute) for the Ratio of means (R_{mean}) indicate that the model predicts the observation with acceptable accuracy (Elias et al. 2006). The negative sign of R_{mean} signifies that the measured values are underestimated in the model (Elias et al. 2006). The index of agreement lies normally between 0 and 1, for good models the value d is higher than 0.6 (Elias et al. 2006).

Table 5. Model performance

	Acetic Acid	Propionic Acid	VFA	COD Reduction	pH
r^2	0.999885381	0.9998249	0.973276561	0.770459797	1
R_{mean}	-0.008952163	-0.009178947	-0.035571244	-0.047208017	0
RMSE	15.24415326	16.50322746	403.0197086	7.028994665	0
d	0.999951274	0.999909903	0.990802021	0.902884454	1

2.4 Summary and Conclusion

The objective of this part of the task was the enhancement of an existing AD model to meet the demands of modelling the biogas process using high concentrated substrates as it is characteristic for a biogas plant working with energy crops. This was achieved by adapting ADM1 (Batstone et al. 2002) from the IWA Task group for Mathematical Modelling of Anaerobic Digestion Processes. This adaptation compromises the implementation of a second hydrolysis rate for carbohydrates and the sulphate reduction process. The so altered model serves also as basis for the VL (D16).

The model was in the first line implemented in Matlab®, Version R2006b, and used as compiled Matlab® script.

The adapted model shows very good results for the simulation of the fatty acid concentration (r^2 0.973) and especially the pH, which is perfectly modelled (r^2 1). Not so good results were found for the prediction of the methane content and the overall gas production (no data shown). Whereas the prediction of the COD reduction also gave good values (r^2 0.770).

Acknowledgement

Special thanks go to C. Rosen and U. Jeppsson for providing the SIMULINK® script of the original ADM1.

References

Amon T, Amon B, Kryvoruchko V, Zollitsch W, Mayer K, Gruber L. 2007. Biogas production from maize and dairy cattle manure-Influence of biomass composition on the methane yield. *Agriculture, Ecosystems and Environment* 118(1-4):173-182.

- Angelidaki I, Sanders W. 2004. Assessment of the anaerobic biodegradability of macropollutants. *Re/Views in Environmental Science and Bio/Technology*(0):1-13.
- Batstone, D. J., J. Keller, et al. (2002a). The IWA Anaerobic Digestion Model No. 1 (ADM1). *Water Sci Technol* **45**(10): 65-73.
- Batstone, D. J., J. Keller, et al. (2002b). Anaerobic Digestion Model No.1. London, IWA Task Group for MAThematical Modelling of Anaerobic Digestion Processes: 50.
- Buffiere P, Loisel D, Berent N, Delgenes J-P. Towards new indicators for the prediction of solid waste anaerobic digestion properties; 2005; Copenhagen, Denmark. p 197-204.
- Chandler JA, Jewell WJ, Gossett JM, Van Soest PJ, Robertson JB. 1980. Predicting methane fermentation biodegradability. *Biotechnology and Bioengineering Symposium* 10:93-107.
- Chynoweth DP, Turick CE, Owens JM, Jerger DE, Peck MW. 1993. Biochemical Methane Potential of biomass and waste feedstocks. *Biomass and Bioenergy* 5(1):95-111.
- Eastman JA, Ferguson JF. 1981. Solubilisation of particulate organic carbon during the acid phase of anaerobic digestion. *JWPCF* 53:253-266.
- Elias, A., G. Ibarra-Berastegi, et al. (2006). Neural networks as a tool for control and management fo abiological reactor for treating hydrgen sulphide. *Bioprocess Biosys Eng* **29**: 129-136.
- Fedorovich, S. V., P. Lens, et al. (2003). Extension of Anaerobic Digestion Model No.1 with Processes of Sulfate Reduction. *Applied biochemistry and biotechnology* **109**: 33-45.
- Hills D, Nakano K. 1984. Effects of particle size on anaerobic digestion of tomato solid wastes. *Agricultural wastes* 10:285-295.
- Hobson P. 1983. The kinetics of anaerobic digestion of farm wastes. *Journal of Chemical Technology and Biotechnology* 33B:1-20.
- Holubar, P., L. Zani, et al. (2003). Start-up and recovery of a biogas-reactor using a hierarchical neural network-based control tool. *Journal of Chemical Technology and Biotechnology*. **78**(8): 847-925.
- Kleerebezem, R. and M. C. M. Van Loosdrecht (2004). Criticizing some concepts of ADM1. Anaerobic Digestion 2004, Montreal.
- Mata-Alvarez J, Macé S, Llabrés P. 2000. Anaerobic Digestion of solid organic wastes. An overview of research achievements and perspectives. *Bioresource Technology* 74:3-16.
- Noike T, Endo G, Chang J, Yaguchi J, Matsumoto J. 1985. Characteristics of Carbohydrate degradation and the rate limiting step in anaerobic digestion. *Biotechnology and Bioengineering* 27:1482-1489.
- Papanastasiou, D. K., D. Melas, et al. (2007). Development and Assment of Neural Network and Multiple Regression Models on order to predict PM10 Levels in a Medium-sized Mediterranean City *Water Air Soil Pollut* **182**: 325-334.
- Pavlostathis, S. G. and J. M. Gossett (1985). A Kinetic Model for Anaerobic Digestion of Biological Sludge. *Biotechnology and Bioengineering* **28**: 1519-1530.
- Sanders W, Veeken A, Zeeman G, Lier van J. 2002. Analysis and optimisation of the AD process of OFMSW. In: J M-A, editor. Biomethanisation of the Organic Fraction of Municipal Solid Wastes. London: IWA publishing. p 63-89.
- Sanders WTM, Geerink M, Zeeman G, Lettinga G. 2000. Anaerobic Hydrolysis kinetics of particulate substrates. *Water Science and Technology* 3(41):17-24.
- Sanders WTM. 2001. Anaerobic hydrolysis during digestion of complex substrates. Wageningen: Wageningen University. 101 p.

- Song H, Clarke WP, Blackall L. 2005. Concurrent microscopic observations and activity measurements of cellulose hydrolyzing and methanogenic populations during the batch anaerobic digestion of crystalline cellulose. *Biotechnology and Bioengineering* 91(3):369-378.
- Song. 2003. Characterisation of microbial community structure within anaerobic biofilms on municipal solid waste [PhD thesis]. Queensland: University of Queensland.
- Strik, D. P. B. T. B. (2004). Modelling and Control of Hydrogen Sulphide and Ammonia in Biogas of Anaerobic Digestion towards Biogas usage in Fuel Cells. Vienna, University of Natural Resources and Applied Life Science.
- Tong X, Smith LH, Mc.Carty PL. 1990. Methane Fermentation of Selected Lignocellulosic Materials. *Biomass* 21:239-255.
- Valentini A, Garuti G, Rozzi A, Tilche A. 1997. Anaerobic degradation kinetics of particulate organic matter: a new approach. *Water Science and Technology* 36(6-7):239-246.
- van Soest PJ, Robertson JB, Lewis BA. 1991. Methods for Dietary Fiber, Neutral Detergent Fiber and Nonstarch Polysaccharides in relation to animal nutrition. *Journal of Dairy Sciences* 74:3583-3597.
- Vavilin VA, Rytov SV, Lokshina L. 1996. A description of the hydrolysis kinetics of particulate organic matter. *Bioresource Technology* 56:229-237.
- Veeken A, Hamelers B. 1999. Effect of temperature on the hydrolysis rate of selected biowaste components. *Bioresource Technology* 69(3):249-255.
- Warren RAJ. 1996. Microbial hydrolysis of polysaccharides. *Annu. Rev. Microbiol.* 50:183-212.
- Wilcox, S. J., D. L. Hawkes, et al. (1995). A neural network, based on bicarbonate monitoring, to control anaerobic digestion. *Water Research* 29(6): 1465-1470.